Reverse Step CFD Analysis

266720[1]

Date: Tuesday 5^{th} March 2024

Abstract

This report is about a numerical investigation of turbulent flow over a backward-facing step using computational fluid dynamics (CFD). The study aims to analyze flow characteristics, including separation, reattachment, and recirculation phenomena, crucial for various engineering applications. The simulation utilizes the Reynolds-Averaged Navier-Stokes (RANS) approach and compares results against Direct Numerical Simulation (DNS) data.

The geometry setup follows specified dimensions, and multiple different meshes were compared and built upon to create a final mesh that captures all the features. In this report, reattachment point was also evaluated.

Despite limitations, including simplifications in fluid properties and unrealistically high initial velocities, the study contributes to advancing our understanding of turbulent flow phenomena.

Nomenclature

ρ	density(kg/m^3)
Cp	Pressure Coefficient
h	0.01m
M	Mach Number
P	Local Pressure (Pa)
P_0	Freestream Pressure (Pa)
Re	Reynolds Number (m/s)
U	Velocity (m/s)
u	Freestream velocity (m/s)
U_0	Initial Velocity (m/s)

Contents

1. DECLARATION

This report, titled: "Reverse Step CFD Analysis", is entirely my own work, unless otherwise acknowledged, and performed under guidance of and for the module of Dr. Mark Puttock-Brown, and the University of Sussex.

2. PROBLEM DESCRIPTION

This problem is a 2D simulation of a backwards facing step using computational fluid dynamics. Turbulent flow over a backward facing step serves as a standard benchmark for validating computational fluid dynamics methods due to its representation of separation, reattachment, and recirculation which will be tested in depth in this report. The geometry will follow Figure 2. With the separation point fixed at the sharp corner over the step, complexities in defining it are avoided. This flow pattern is prevalent in various engineering applications and extensively studied in both experimental and numerical contexts. ANSYS Workbench is used for the geometry construction, grid generation, and FLUENT for flow solution. This report also invents a theoretical fluid of density and dynamic viscosity = 1 to give easier numbers. This report presents a numerical investigation of turbulent flow over a backward-facing step using the Reynolds-Averaged Navier-Stokes (RANS) approach. The analysis will involve comparing results against Direct Numerical Simulation (DNS) data.

3. LITERATURE REVIEW

This report's literature review revolves mostly around Kopera et al., 2014, which is also a report about CFD across a backward facing step (BFS).

Le et al. (1997) conducted Direct Numerical Simulation (DNS) studies, offering valuable data on separation, recirculation, and reattachment phenomena near the step. Kopera et al. (2014) extended this work, exploring diverse flow parameters and configurations through DNS simulations.

Benchmark experimental data by Kim et al. (1987) and Moser et al. (1999) allowed for of DNS results, particularly concerning velocity profiles and turbulence characteristics. Computational methodologies have changed, using advanced numerical techniques and parallel computing for more accurate simulations. This has allowed for more circulations to be added and a more accurate reattachment point.

Comparisons between DNS outcomes and theoretical models has helped the understanding of BFS flow dynamics, integrating experimental data, theoretical frameworks, and numerical simulations. All of these have helped with the theory behind this report.

4. SETUP

4.1. Geometry

The geometry, shown in Figure 1 is essentially as specified in the brief, shown in Figure 2, where h=0.01m and $L = h \times 10$. The density and dynamic viscosity of the fluid in the fluid domain has been defined in this simulation as 1 which means that:

$$Re = U_0 \times h = 5100, \tag{1a}$$

$$\frac{5100}{0.01} = U_0 = 51,000 m/s \tag{1b}$$

This is, obviously, way too fast and will decrease immediately upon entering the fluid domain.

4.2. Mesh

4.2.1. Initial

For the initial mesh, seen in Figure 3, the method was quadrilateral dominant, and the element size was 0.002m. This has created about 4000 elements. This is a very rudimentary mesh and is only used to confirm the theory. Future meshes should and will be more concentrated around areas that that the results show our of interest.

4.2.2. Second

With the second mesh, seen in Figure 4, the all triangle method of automatic mehing was used, and the element size was 0.002m. We also added inflation around the edges to refine the areas that are shown

*Kopera, M.A., Kerr, R.M., Blackburn, H.M. and Barkley, D. (2014). Direct Numerical Simulation of Turbulent Flow over a Backward-facing Step. J. Fluid Mech, pp.1–24.

†Le, H, Moin, P. & Kim, J. 1997 Direct numerical simulation of turbulent flow over a backward-facing step. Journal of Fluid Mechanics

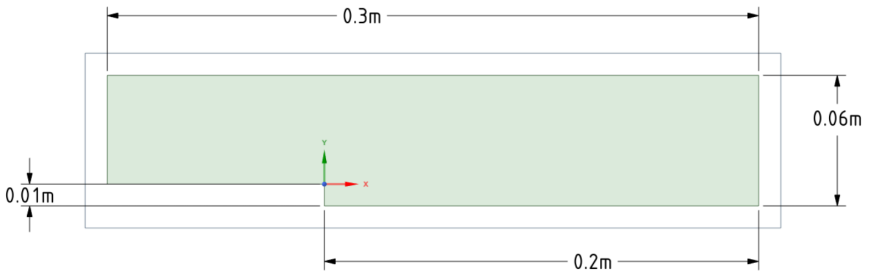

Fig. 1: Geometry of the problem in ANSYS

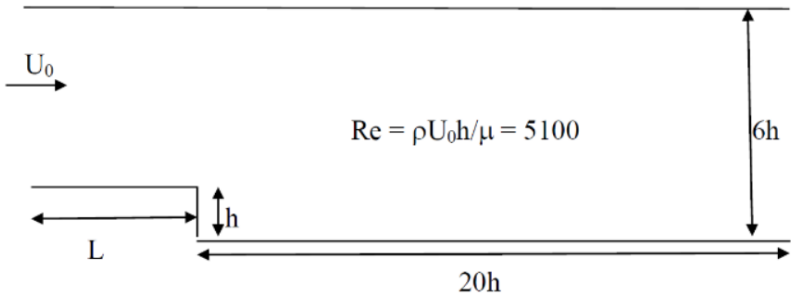

Fig. 2: Backwards Facing Step - Solution Domain

to have 'features of interest' by Figure 4. This has created about 10000 elements. This mesh was concentrated around all the wall regions to make sure that the regions around the wall was refined and better results could be obtained.

4.2.3. Third

The method to generate the third mesh, which is also shown, this time in Figure 5, instead uses sphere of influence and the all triangles method to create it. From this moment on, in this report, the meshes are all built with sphere of influence. It was used to have a small look into what the sphere of influence can do and was not the most refined mesh, this only created around 10000 elements too. The Sphere of influence has a radius of 0.05m.

4.2.4. Fourth

For this Mesh, shown this time in Figure 6 it has been built with a smaller sphere of influence to more refine the area that this report is focusing on: the step. There is also now a greater amount of elements in the sphere of influence, the entire mesh is now 60000 elements.

4.2.5. Final

In the Fifth mesh, shown in Figure 17, edge sizing was used along the bottom edge to insure that the reattachment point is accurate, and then a sphere of influence to catch the rest of the features including where the eddy circulates. Within both these features the element sizing is 0.0002m which makes the final number of elements 61696.

5. ANALYSIS

5.1. Analysis of initial results.

The velocity vectors shown in Figure 8 show where the mesh needs to be refined. In figure 8 it shows that the mesh needs to be refined in the area where we have an eddy forming especially in the centre and in the separation zone where the flow makes contact with the wall and further into the corner where a reverse of the circular flow should be the happening.

5.2. Analysis of Second Mesh

The second attempt, results shown in Figure 9 and 10, show that the refinement captures all the features that want to be seen. This is quite a good mesh because of this.

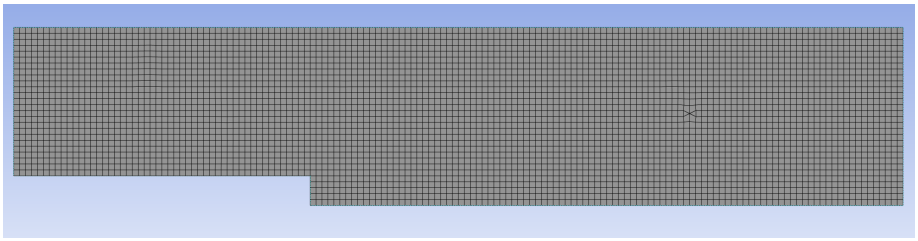

Fig. 3: Initial Mesh in ANSYS

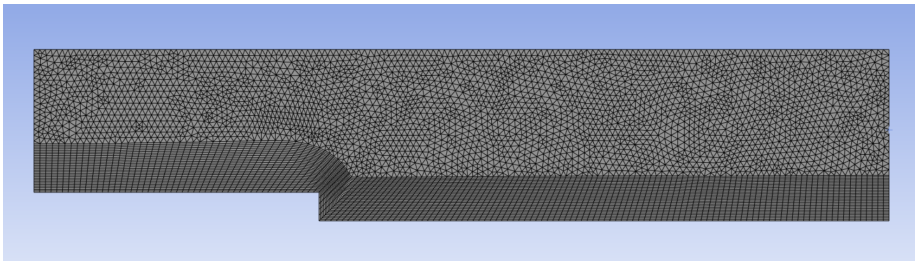

Fig. 4: Second Mesh in ANSYS

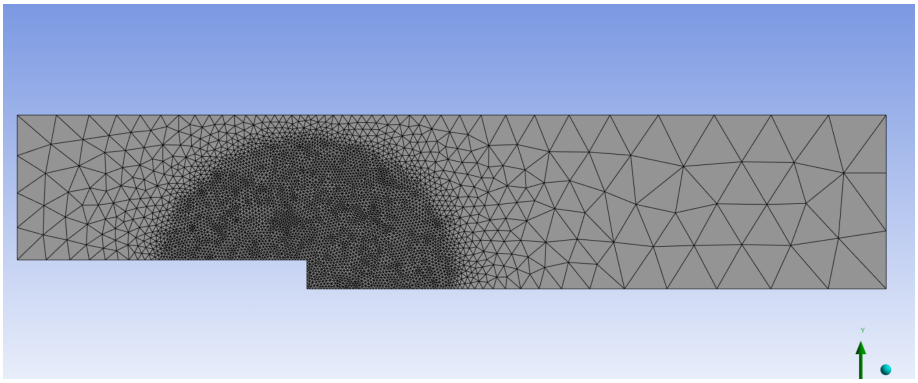

Fig. 5: Third Mesh in Ansys

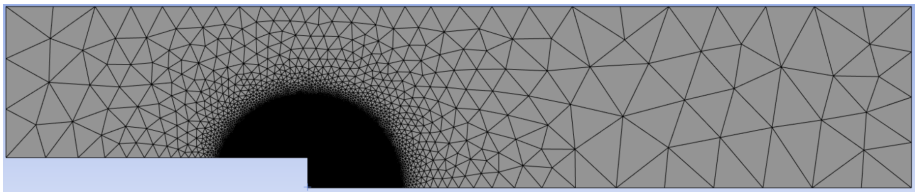

Fig. 6: Fourth Mesh

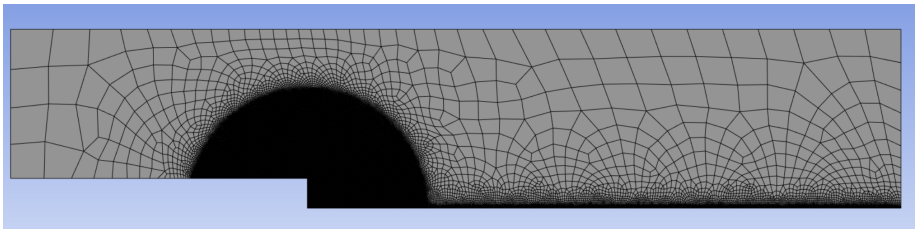

Fig. 7: Final Mesh

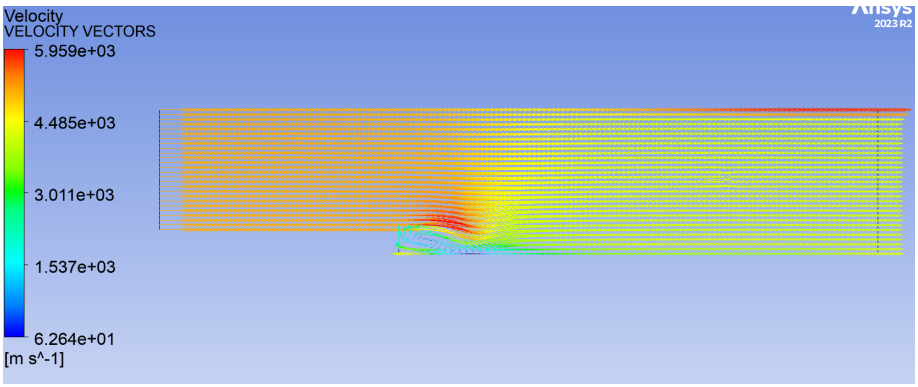

Fig. 8: Initial velocity vectors in ANSYS

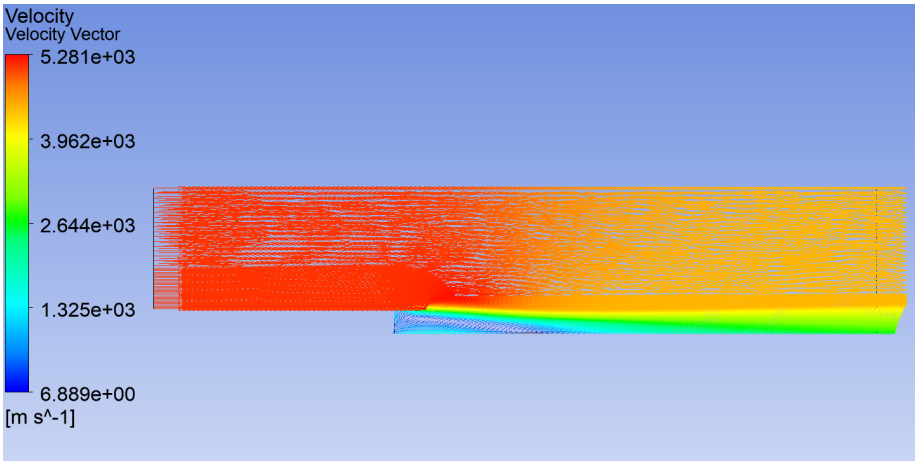

Fig. 9: Second attempt velocity vectors in ANSYS

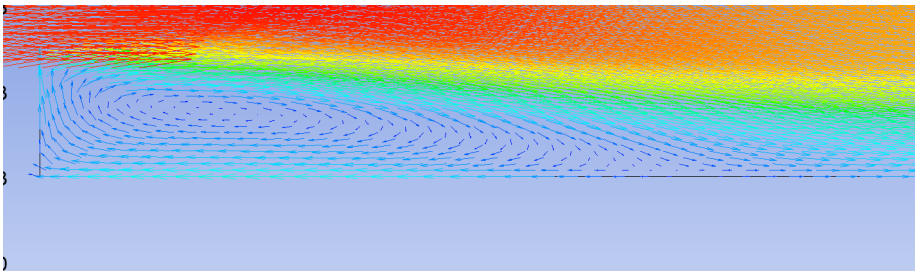

Fig. 10: Second Attempt velocity vectors in ANSYS zoomed in

5.3. Analysis of Third Mesh

Third mesh had to use a smaller initial velocity because otherwise it wouldn't fit in the sphere. 5100m/s was used instead. The results are shown in Figures 11, 12, and 13.

5.4. Analysis of Fourth Mesh

As seen in Figure 16, the radius of the sphere of influence is too small to truly capture the reattachment point. For the next attempt, the radius must be increased. Figure 14 and 15 show the pressure contours of the which follow the same as Figure 11 and 12 in the third mesh and shows a lack in pressure just behind the step and an increase in pressure just above the step, which is what should be expected of theory of separation of laminar flow, which is what is being modelled.

5.5. Final mesh Analysis

For this mesh we have captured every point, and so this is the final design all future analysis sections will be based around this mesh. The reattachment point is caught by the edge sizing, as seen in Section 8: Reattachment point, and the rest is caught by the sphere of influence. Results are shown in Figure 17, 18, and 19

6. U_0/U ANALYSIS

At x/h=15, shown in Figure 16, the velocity profile displays non-uniformity, characterized by a steep gradient near the step. This non-uniformity shows that the flow will circulate back on itself once past the step, which can significantly influence the overall flow behavior and efficiency. However, at x/h=6, this time shown in Figure 20 the velocity profile exhibits much greater uniformity, with velocity remaining relatively constant across the flow cross-section. This indicates that the flow has fully recovered from the step's effects, and the downstream region offers a more representative perspective of the overall flow behavior without the step's interference. The uniform velocity profile in the downstream region also implies that it is a suitable location for assessing the flow system's overall performance.

If compared to the simulated data with the DNS data provided in the brief, the maximum velocity profile value from the DNS data closely resembles the simulated data for both graphs. However, it reached its peak much later than the simulated model, suggesting that the simulated model predicts a thinner boundary layer compared to the DNS results. Furthermore, while the simulated model reached its peak but slightly dropped in value immediately afterward, the DNS graph maintained its maximum value once reached.

7. K/U_0^2 ANALYSIS

At x/h=15, shown in Figure 22, the K/U_0^2 variable exhibits a significantly smaller value compared to x/h=6, shown in Figure 23. When comparing it to the DNS values at x/h=15, we would anticipate the simulated graph to display a larger maximum value, especially considering that some initial data points were omitted, rendering our graph somewhat inaccurate.

Similar to the U/U_0 graphs, both simulated graphs plateau much earlier compared to the DNS graphs, aligning with our previous analysis and supporting the notion of a thinner predicted boundary layer.

The comparison between the velocity profiles at x/h=6 and x/h=15 underscores the importance of selecting an appropriate downstream location for measuring the flow system's overall performance. The non-uniformity of the velocity profile near the step suggests that assessing performance at this location may not offer a representative view of the flow behavior. Conversely, the more uniform velocity profile in the downstream region implies that this location provides a more precise measure of the flow system's overall performance.

8. REATTACHMENT POINT

For the reattachment point, the final mesh can be used because it offers detail along the bottom edge due to edge sizing the mesh, with the correct velocity to match Reynolds number. The reattachment point was calculated by finding the closest value to zero along the bottom edge. The most accurate reading is at 0.0721533m away from the step where the fluid is moving at 0.038826m/s. These are shown in Figure 24.

9. DISCUSSION

9.1. Velocity and Pressure Analysis

The analysis of velocity vectors and pressure contours indicated regions of interest; areas of separation, reattachment, and eddy formation. The non-uniformity of velocity profiles near the step suggested the presence of circulation zones, while pressure contours highlighted variations in flow behavior across different mesh configurations. This would have had more accurate results had the chosen properties been for a fluid that exists.

9.2. Reattachment Point

Determination of the reattachment point, a critical parameter in BFS flow analysis, was conducted. The

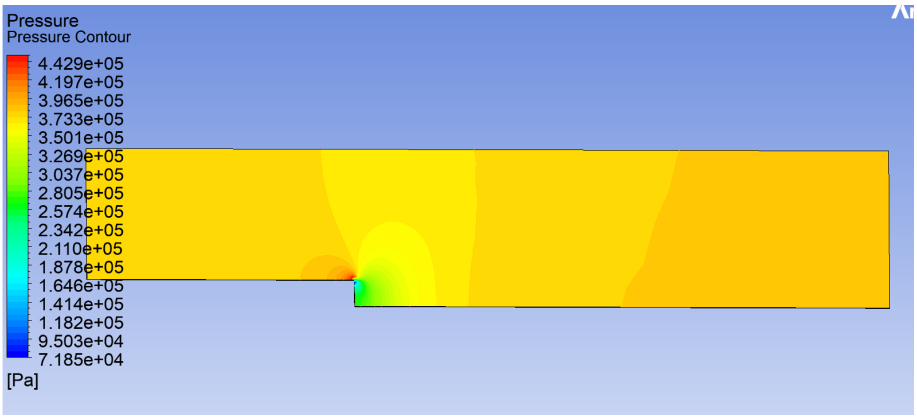

Fig. 11: Third Attempt Pressure Contour

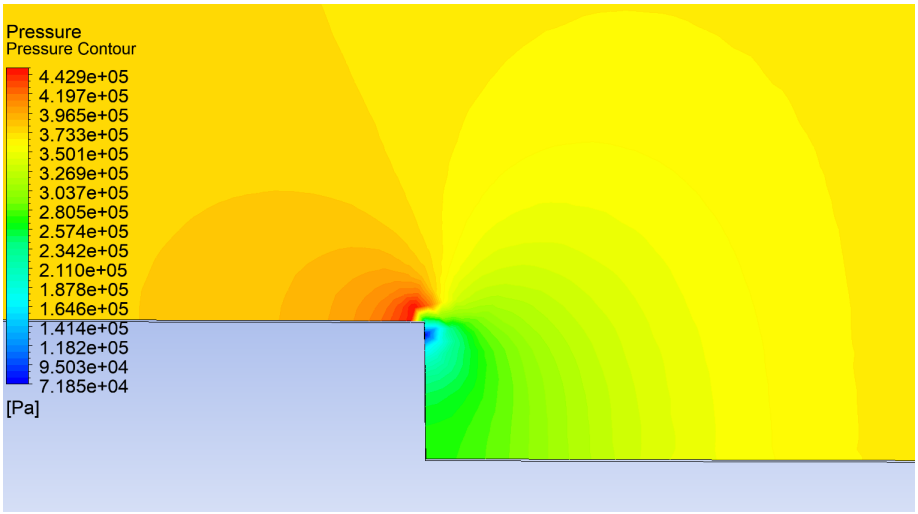

Fig. 12: Third mesh pressure contours in ANSYS zoomed in

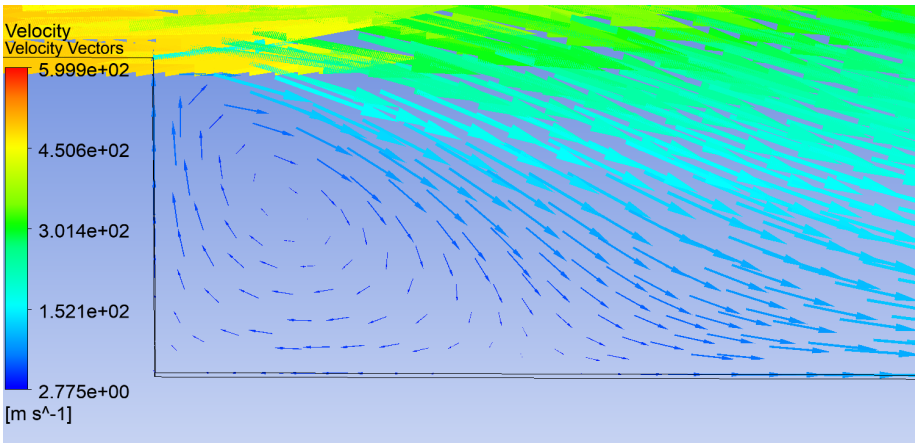

Fig. 13: Third attempt velocity vectors in ANSYS zoomed in

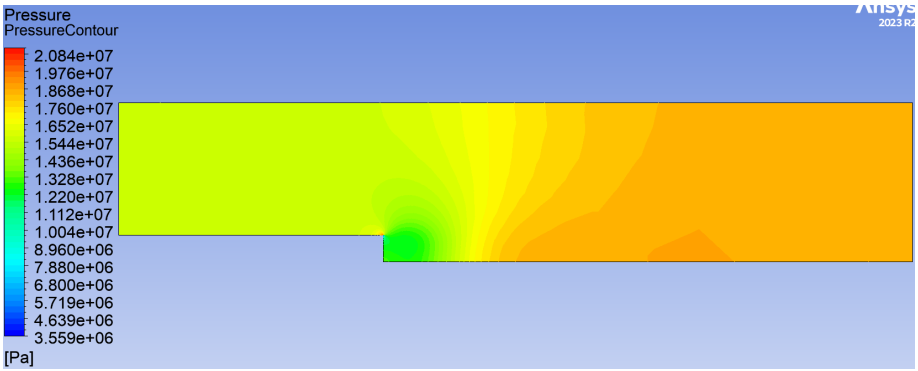

Fig. 14: Fourth mesh pressure contours in ANSYS

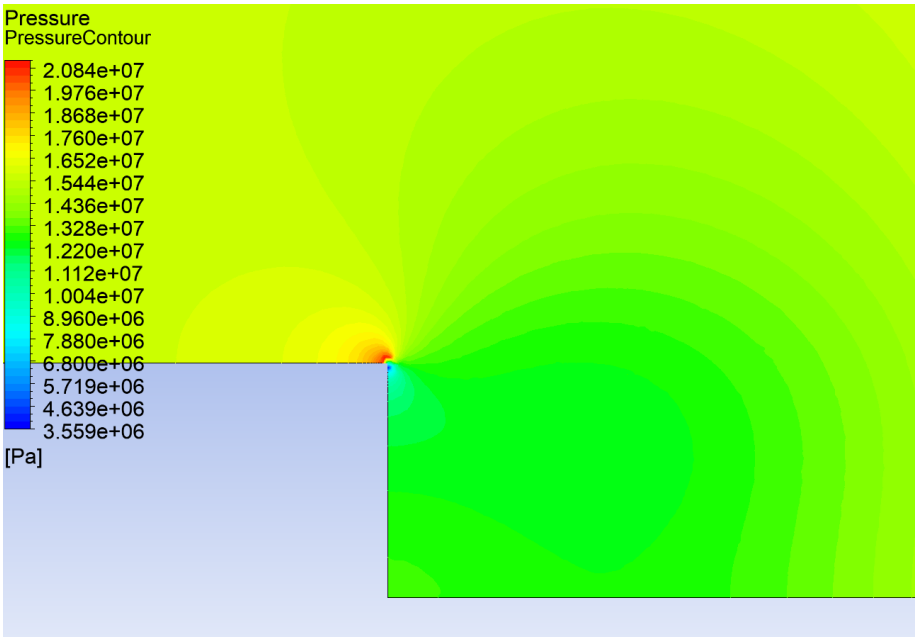

Fig. 15: Fourth mesh pressure contours in ANSYS zoomed in

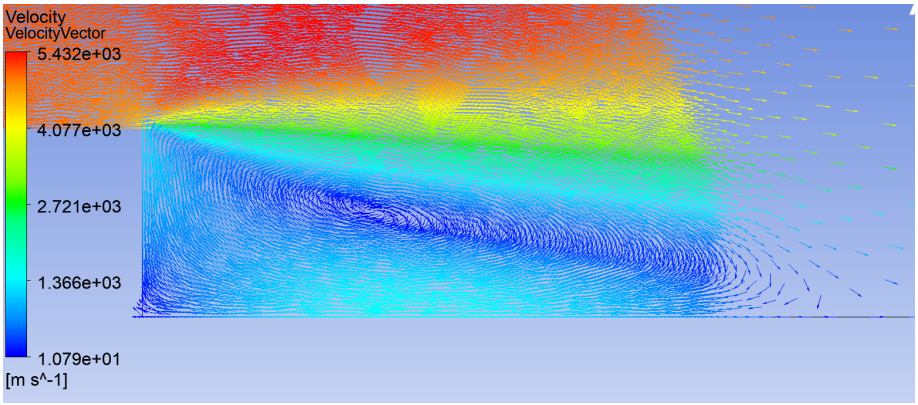

Fig. 16: Fourth attempt velocity vectors in ANSYS zoomed in

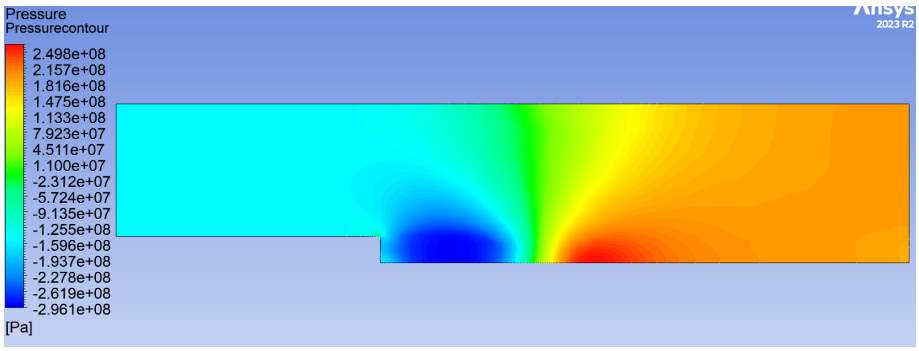

Fig. 17: Final mesh pressure contours in ANSYS

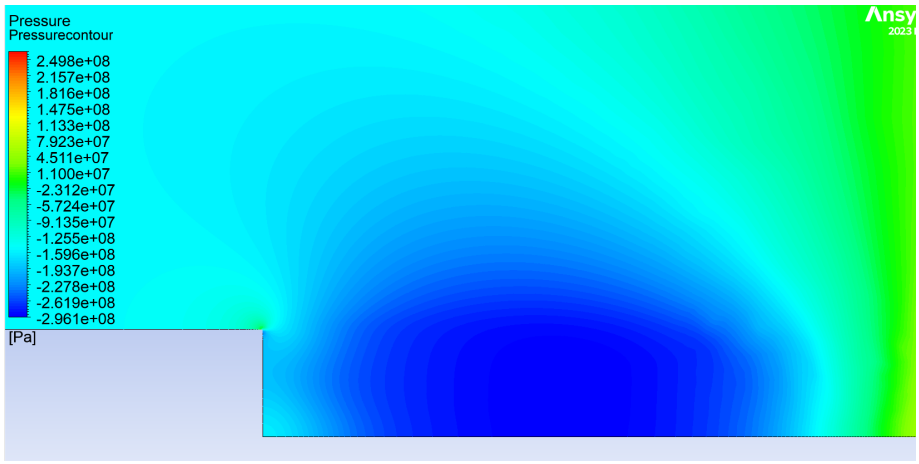

Fig. 18: Final mesh pressure contours in ANSYS zoomed in

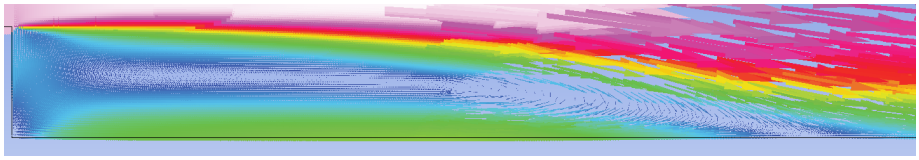

Fig. 19: Final velocity vectors in ANSYS zoomed in

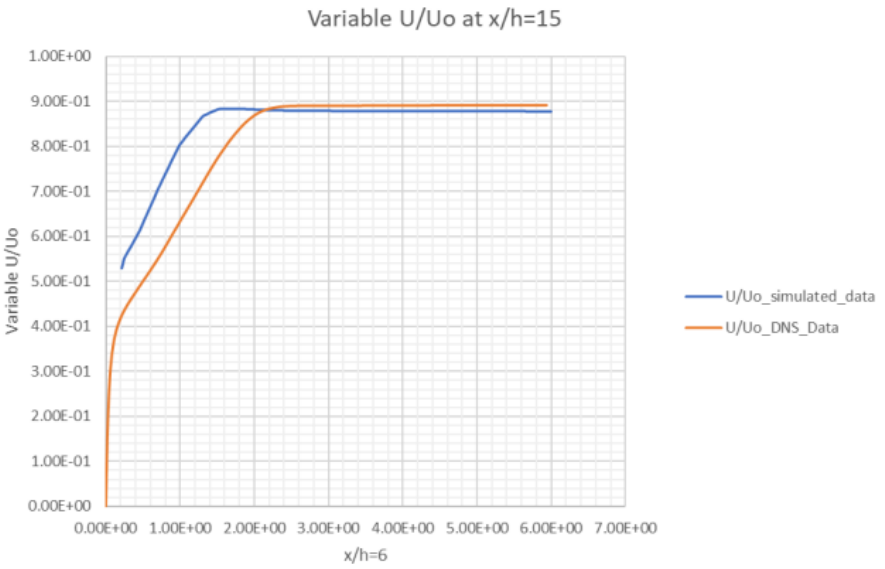

Fig. 20: U_0/U at x/h=15

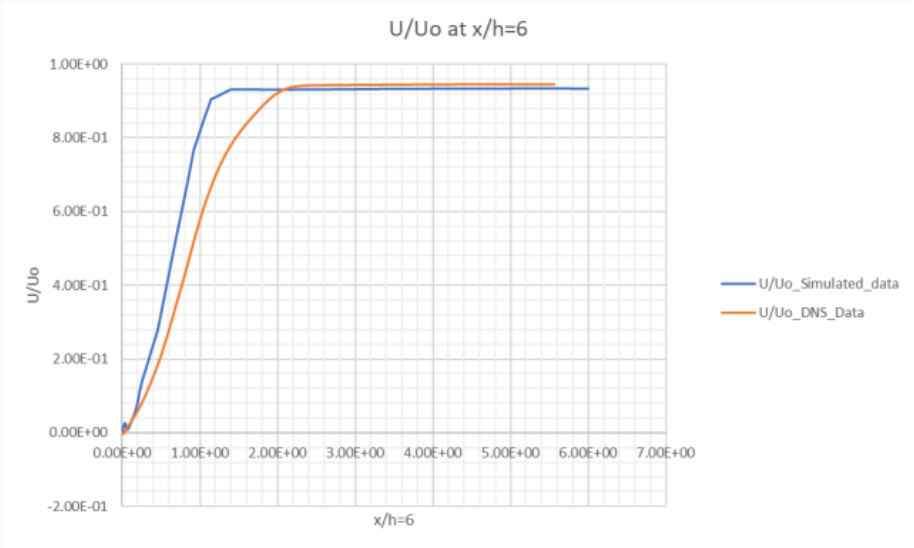

Fig. 21: U_0/U at x/h=6

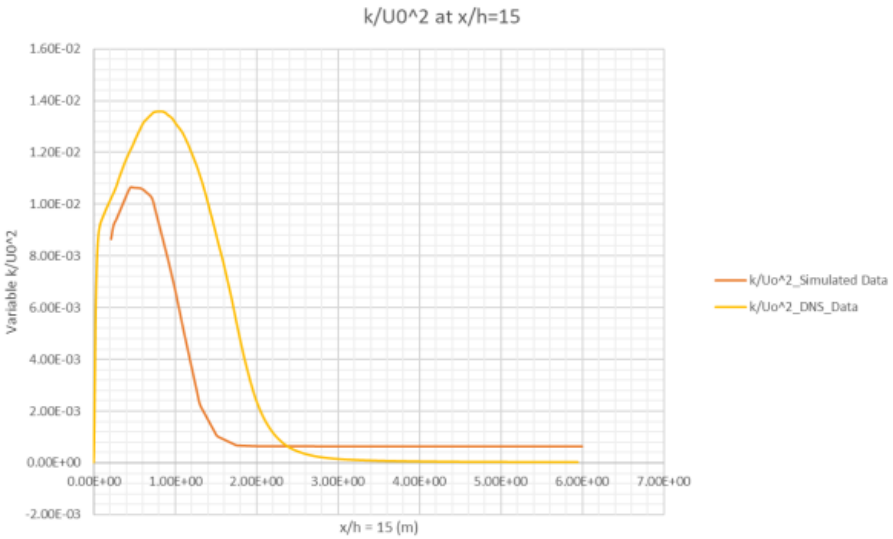

Fig. 22: K/U_0^2 at x/h=15

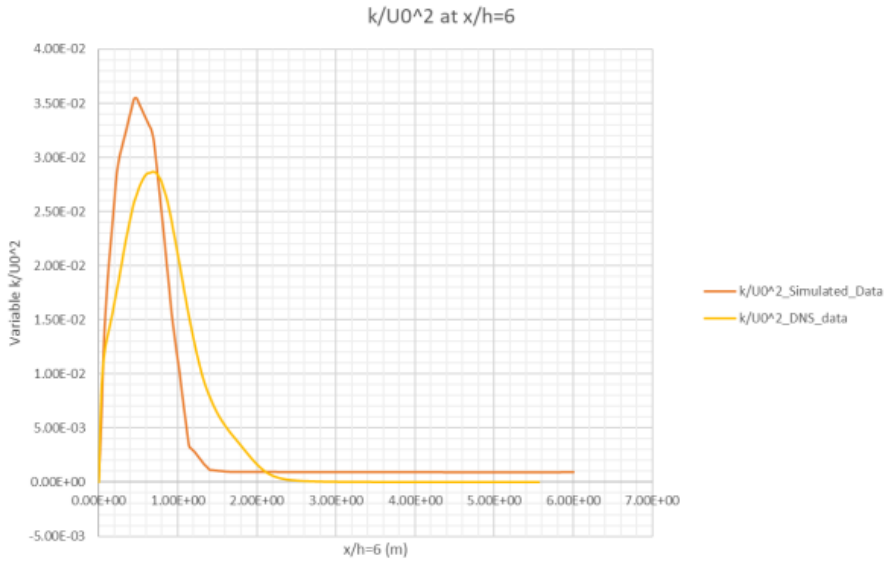

Fig. 23: K/U_0^2 at x/h=6

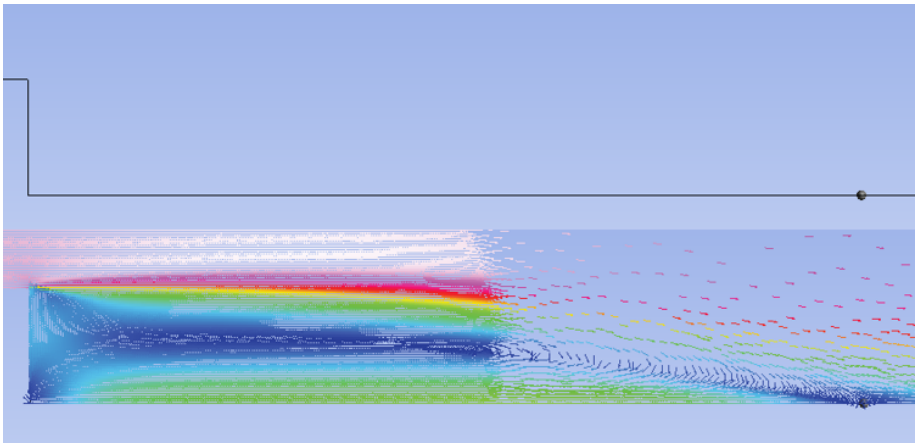

Fig. 24: Reattatchment point with and without velocities done with final mesh